

# COMPUTATIONAL SIMULATION OF FAST-RESPONSE SOLENOID ACTUATOR OF ENGINE FUEL SYSTEMS

Leonid Grekhov,  
Bauman Moscow State Technical University,  
BMSTU, Moscow, Russia,  
lgrekhov@mail.ru

Jianhui Zhao, Xiuzhen Ma  
Harbin Engineering University,  
HEU, Harbin, China  
zhaojianhui@mail.ru

**Abstract --** Performance of the fast-response solenoid actuator of the engine fuel systems is characterized with a response time of less than 0.1 ms and necessity to take the nonstationary peculiarities of mechanical, hydraulic, electrical and magnetic processes into consideration. For this purpose, simple models are used for magnetizing within the static and dynamic hysteresis, nonstationary electrical process in the capacitor-fed circuits, and hydromechanical processes in the electro-hydraulic injector of the Common Rail fuel systems. The experimental study of the actuator performance within the electro-hydraulic injector of the diesel engine demonstrated agreement between the computational and experimental results. Thus, computational modeling is a tool for analysis, as well as a tool for design and optimization of the solenoid actuator. Using the integral actuator performance model within the software for computation of the engine fuel equipment allows, as a result of its optimization, achieving the best performance of the fuel system, and with low engine emissions and low fuel consumption.

**Keywords—** Diesel Engine, Fuel System, Solenoid Actuator, Mathematical modeling, Nonstationary process

## I. INTRODUCTION

The authors propose utilization of a simple and convenient method for computation of the magnetization curves and static hysteresis loops in a logarithmic form. For the initial magnetization line (for the O-A area, Fig. 1), the connection between magnetic flux density  $B$  and magnetic field intensity  $H$  is represented as:

$$B = 1/a \cdot \lg^c [H/H_c + 1] \quad (1)$$

For the static hysteresis loops (Fig. 1):

$$B = \begin{cases} 1/a \cdot \lg^c [H/H_c + 2] & \text{for A-C area} \\ -1/a \cdot \lg^c [-H/H_c] & \text{for C-D area} \\ -1/a \cdot \lg^c [-H/H_c + 2] & \text{for D-E area} \\ 1/a \cdot \lg^c [H/H_c] & \text{for E-A area} \end{cases} \quad (2)$$

The  $C$  and  $a$  constants may be determined based on scarce reference data. If the reference data on  $B_m(H_m)$ ,  $H_c$ ,  $B_r$ , are available, the  $C$ ,  $a$  coefficients can be determined as follows:

$$C = \lg (B_m/B_r) / \lg \left[ \frac{\lg (H_m/H_c + 2)}{\lg 2} \right]; \quad (3)$$

$$a = \lg^c (H_m/H_c) / B_m.$$

If any data on the material  $B_m(H_m)$ ,  $H_c$ ,  $\mu_{max}$ , are available,  $\mu_{max}$  is referred to the  $B \rightarrow 0$  neighborhood:

$$\mu_{max} = \frac{dB}{dH} \approx \frac{B}{\Delta H} = \lg^c \left( \frac{\Delta H}{H_c} + 1 \right) / a \cdot \Delta H. \quad (4)$$

$$C = \lg \left( \frac{B_m}{\mu_{max} \cdot \Delta H} \right) / \lg \left[ \frac{\lg (H_m/H_c)}{\lg (\Delta H/H_c + 1)} \right] \quad (5)$$

$$a = [\lg (H_m/H_c)]^c / B_m.$$

The effectiveness of such approximation was proven by comparison the results of calculations in accordance with (1)-(2) with the known experimental results and own experiments. It remains possible to directly use the experimentally obtained  $B=f(H)$  bulk data. However, using the (1)-(5) dependences not only accelerates counting but also increases the model universalization with respect to the materials for which such detailed information is not available. Approximation (2) provides agreement with the experimental data for the steels that are used in FRSA. The ignored curve bend in the event of the initial magnetization in the low value range of the flux density for the FRSA is minor due to a very short period of time and narrow hysteresis loop for the materials used. The applied values of  $B_r$ ,  $B_m(H_m)$ ,  $H_c$ ,  $\mu_{max}$  are the ordinary reference parameters of the magnetic material and, therefore, the (1)-(5) relations are convenient for use.

The next stage of the FRSA mathematical simulation is its study and design optimization, including the latest approaches to the problems [1].

Furthermore, for the fast-response solenoid actuator (FRSA) with a response of 0.1 ms and less, specific nonstationary electromagnetic processes become relevant. These include delayed FRSA action due to remagnetization of the material (magnetic viscosity) and occurrence of eddy currents in the magnetic core. For description of the dynamic hysteresis, we use the model of A.I. Kadochnikov [2], [3]. It is a semi-empirical model characterized with a simple and adequate description of the most important nonstationary remagnetization effects. The effective field intensity with the same flux density exceeds the quasi-static one:

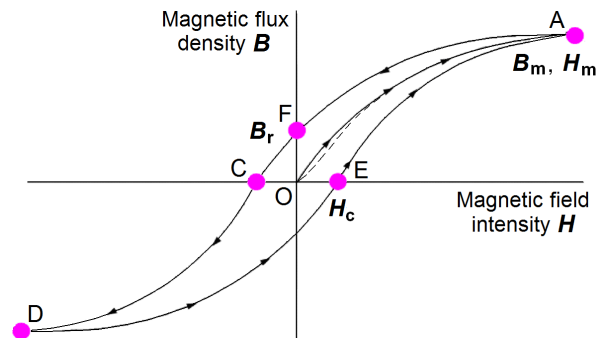


Fig. 1. Scheme of static hysteresis

$$H_d(t) = H_{st}(B_{av}) + \frac{1}{r} \exp\left(\alpha \frac{B_{av}^2}{B_m^2}\right) \cdot \frac{dB_{av}}{dt} + \frac{1}{3} \gamma_{eq} \delta^2 \cdot \frac{dB_{av}}{dt}, \quad (6)$$

where:  $\delta$  - one-half thickness of the strip of the imbricated plates;

$H_{st}(B_{av})$  - static remagnetization curve;

$H_d$  - dynamic field intensity considering the consumption for remagnetization;

$r$  - magnetic viscosity coefficient characterizing dynamic interaction of the domain walls with restrictions when remagnetizing;

$\alpha$  - magnetic viscosity parameter depending on the material composition and manufacturing technology;

$\gamma_{eq} = \lambda \cdot \gamma$  - equivalent specific conductivity of the magnetic material;

$\gamma$  - real specific conductivity of the magnetic material;

$\lambda$  - characteristic of the domain structure fragmentation degree.

The  $\alpha$ ,  $\gamma_{eq}$ ,  $r$  coefficients and dependences for their determination are given for popular electrotechnical steels in [2] based on the experimental studies.

## II. SIMULATION OF FRSA PERFORMANCE FOR ENGINE FUEL SYSTEMS

The described dependences enabling the  $H=f(B)$  relations for the magnetic core are further used to determine the force generated by the FRSA. For this purpose, in the applied algorithm, the magnetic flux  $\Phi$  is determined as follows:

$$\Phi = \frac{iw}{R_{cl} + R_{core}} = iw \left/ \sum_{i=1}^2 \frac{\delta_{cl-i}}{S_{cl-i} \cdot \mu_f} + \sum_{j=1}^k \frac{l_{core-j}}{S_{core-j} \cdot \mu_{core}} \right. \quad (7)$$

where:  $i$  - current;

$w$  - number of the winding turns;

$\delta_{cl}$  - operating clearance;

$\mu_f$  - fuel magnetic permeability ( $1,2566 \times 10^{-6} \text{ GH/M}$ );

$l_{core}$  - length along the magnetic core median line;

$S_{cl}$  - operating clearance cross-section area;

$S_{core}$  - magnetic core cross-section area.

The total magnetic resistance  $R_{\Sigma} = R_{cl} + R_{core}$  can be calculated along the magnetic flux line with the equivalent length and cross-section. The complex law of the instantaneous current variations in the coil circuit is considered to be known if it is directly preset by the control system. If the control system forms the known voltage variation law, the current is calculated based on the models for the capacitor-fed electrical circuits and coil flux density available (Fig.1, right branch) [3].

$$\frac{di}{dt} = \frac{1}{L} \left[ E_0 - \frac{1}{C} \int_0^t i dt - iR - i \frac{dL}{dt} \right] \quad (8)$$

where:  $i$  - current;

$E_0$  - initial EMF of the source;

$R$  - active resistance;

$C$  - capacity of pulse capacitor;

$L$  - FRSA flux density.

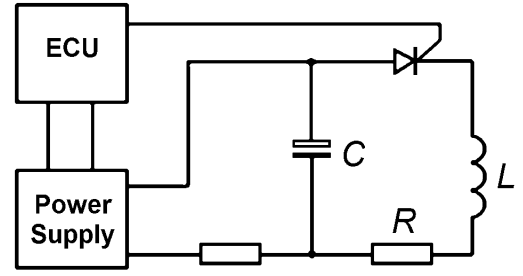


Fig. 2. Electrical circuit of FRSA supply circuit replacement

$$L = w^2 \left/ \left( \frac{2\delta_{cl}}{S_{cl} \cdot \mu_f} + \frac{l_{core}}{S_{core} \cdot \mu_{core}} \right) \right.$$

The field intensity  $H_{core}$  in the magnetic core with a constant cross-section is determined through the magnetic flux  $\Phi$ :

$$H_{core} = \Phi / S_{core} \cdot \mu_{core} \quad (9)$$

The force acting in the solenoid actuator, considering the  $k_{scat}$  coefficient of the magnetic flow scattering:

$$F_{FRSA} = B_{cl}^2 \cdot S_{cl} / \sqrt{k_{scat} \cdot \mu_f} \quad (10)$$

The given FRSA model is used for description of the forces acting on the control valve of the electro-hydraulic injectors of the Common Rail system. To examine performance of the fuel system as a whole, the INJECT software is used. The hydrodynamic fuel system simulation tool INJECT has been designed and experimentally validated by one of the authors of this article, L.Grekhov, Professor of BMSTU [4]. The processes in the fuel systems are described based on the well-known original author's models [5].

## III. COMPUTATIONAL AND EXPERIMENTAL STUDY OF FAST-RESPONSE SOLENOID ACTUATOR PERFORMANCE WITHIN COMMON RAIL INJECTORS

After identification based on the FRSA static characteristics, comparison of the computational and experimental results with real-time changes of the control current was of interest to the authors. Fig. 3 shows the executive software window in which the dependences of the current and valve stroke are displayed when the experiment is carried out in the described test bed. There is a possibility of a random shaping of the control diagram for the current within their reasonable limitations.

For illustration, the FRSA operation mode is taken with an intermediate level of the holding current after the afterburning area and main level of the current holding the anchor in operation condition (Fig. 4). When computations were performed in the ANSOFT Maxwell software, the control current diagram was preset directly by range domain. When working in the INJECT software, schematization of the diagram by the main areas was used for more efficient work (Fig. 4).

The computation results of the FRSA processes were compared with the experimental data obtained in the test bed built by Electronic Control Institute of Power Plant at Harbin Engineering University. In the operating area of the test bed, the electro-hydraulic injector was installed. The test bed comprises an auxiliary hydraulic system with a high pressure pump, an electronic control system, and a system for measuring the electrical, mechanical and hydraulic parameters.

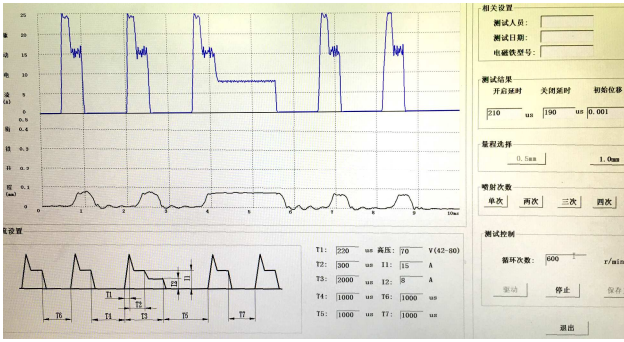


Fig. 3. Window of executive software which controls test bed performance, showing results of current and valve stroke recording

Fig. 5 shows the computational and experimental curves for the control valve lifting with the FRSA anchor in the time function. The computations were performed when using both the ANSOFT Maxwell software and described procedure, which is utilized in the INJECT software.

The zero line in the experimental curve below zero and the stroke above 0.7 mm are determined by the measuring technology and actual valve stroke in the FRSA under examination.

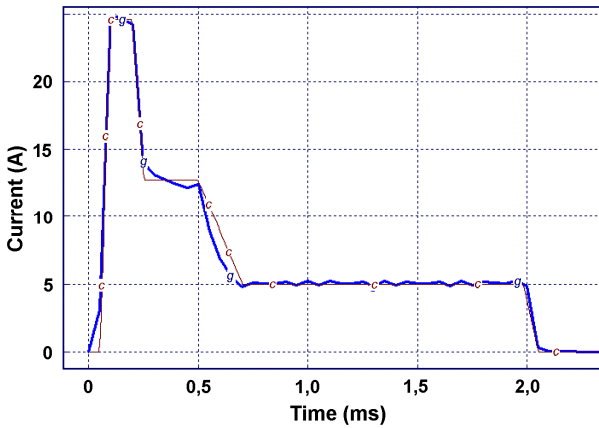


Fig. 4. Time-variation of control current when studying FRSA performance under nonstationary conditions in the simulation test bed: a - experimental values; b - approximation of experimental values when presetting in INJECT

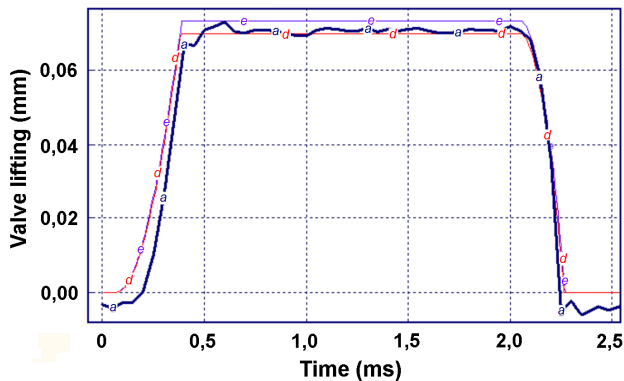


Fig. 5. Control valve lifting in the time function with control current acting as in Fig.4: a - experimental values; c - computation in ANSOFT Maxwell; d - computation in INJECT

It is obvious that the results of the computations by means of two different software tools are practically identical. An advantage of the ANSOFT Maxwell software is the possibility of more accurate computation of the magnetic core of random geometry. On the other hand, the optimized geometry with constant cross-section along the length of the magnetic flux lines is of interest to the authors. Presetting of the magnetic core as the piecewise-constant areas in the INJECT software satisfies this condition. However, the main advantage of the INJECT software is the opportunity to analyze the FRSA performance within the whole fuel system and its optimization for improvement of the fuel injection quality. Therefore, the INJECT software becomes applicable for optimization and design of the fuel system with the FRSA of the control valve.

Under the conditions of the fast nonstationary process, the FRSA behaviour has its own specific features. Magnetic resistance of the clearance and magnetic core depend on the instantaneous value of the valve position, instantaneous magnetic intensity, magnetization rate. These include both the current change under an unspecified law and field intensity considering the dynamic magnetic processes. For these reasons, unlike with the resistance ratio under the static magnetization in the fast process, the picture is more complex (Fig. 6).

The FRSA flux intensity depends not only on the mode parameters – current and magnetic saturation approach, but also on the current valve lifting, i.e. the value of the operating clearance, i.e. magnetic resistance of the clearance and magnetic core. In the dynamic hysteresis, the flux intensity is influenced by the dynamic magnetic effects as well (Fig. 7).

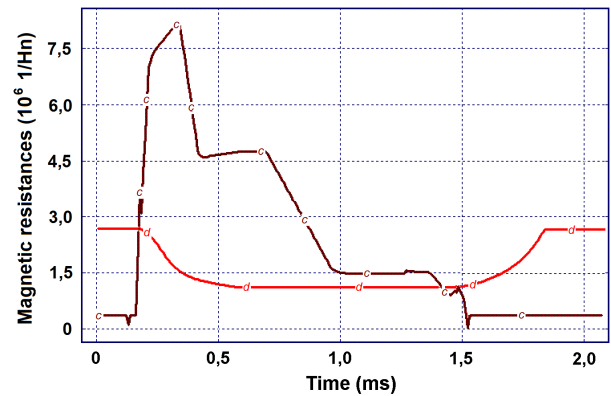


Fig. 6. Magnetic resistances of FRSA: magnetic core (c) and operating clearance (d) in fast fuel injection process.

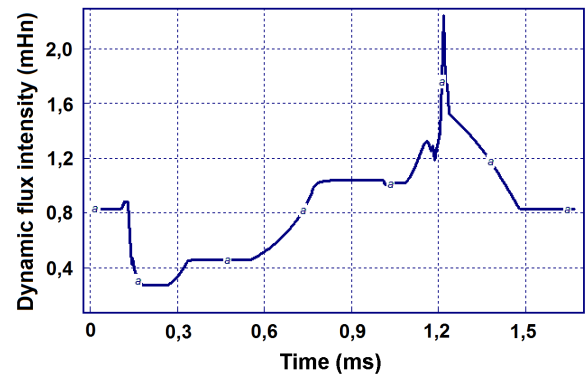


Fig. 7. FRSA dynamic flux intensity in fast injection process

#### IV. STUDY OF FRSA PROCESS WITH INCOMPLETE DEMAGNETIZATION OF MAGNETIC CORE

The classical diagram of the FRSA control, which was shaped at the end of the last century, comprises a phase of the forced feed, a phase of anchor holding in operation condition, and a phase of demagnetization (Fig. 8) [5]. The INJECT simulation of the process enables simple conclusions on the FRSA control law  $U=f(t)$  or  $I=f(t)$ . Thus, afterburning may help near magnetic saturation and, seemingly, its amplitude is unreasonably heightened. However, its importance does not lie only in generation of a stronger force but in accelerated achievement of the force.

Less known FRSA control methods should be briefly mentioned as well. If a sufficient current is reached due to afterburning, no feed may be provided at the second stage – holding, especially for incomplete fuel injections. Recently, as opposed to the diagram in Fig. 8, the diagram with two holding voltage (current) levels has been used – Fig. 4.

From the point of view of the control valve behavior, it is not necessary and, as both computation and experiment show, does not influence the FRSA behavior and the valve affected by it. Comparison of the control scenarios with one level and two levels of the voltage and holding current (Fig. 9) indicates that with two holding levels there is a possibility to support the anchor movement when it has already gained sufficient speed and to prevent the anchor fluctuations on the support, if any. The valve behavior with one holding level and compensation of the first holding level with the 30%-extended afterburning is the same. The energy consumption for the cycle is the same and may be lower. Thus, for the equal valve movement, the average power for the engine operation cycle decreased from 1,064W to 1,035W (correspondingly, the cycle heat release decreased from 0.06387 to 0.06208 J). However, utilization of two holding levels may be motivated by reduced energy consumption for the forcing feed phase.

The final phase of the FRSA feed process is usually called demagnetization. The unconditional purpose of this stage is fast current reduction to zero, and cessation of magnetic core magnetization (the solid line at the end of Fig. 8). However, in accordance with Fig. 1, with zero magnetic field intensity, it is possible to keep residual magnetization and slow down closing of the control valve. Reduction of the fast response of the valve and injector as a whole impedes the operating process of the diesel engine.

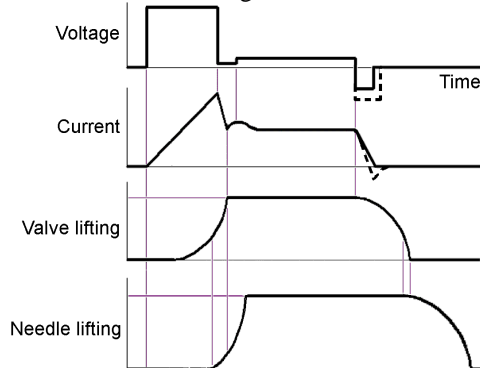


Fig. 8. Classical diagram of source voltage control

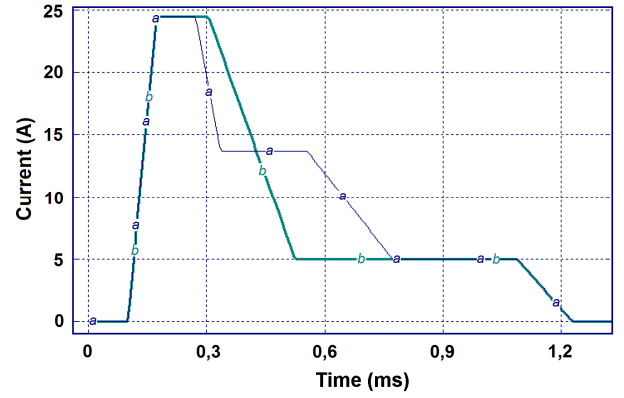


Fig. 9. Time-variation of control current when FRSA performance is studied in nonstationary conditions in the test bed when computing in INJECT: a – two levels of holding current; b – one level of holding current

Description of the complete demagnetization may require all Formulas (2). The optimized process follows the hysteresis trajectory: O-A-C-O (Fig. 1). For complete demagnetization, very insignificant reduction of  $H$ , less than  $(-H_c)$  is possible. However, if the  $H$  reduction is limited to zero, it does not ensure remagnetization of the magnetic core and reduces the interval of force changing from the initial status to the operating condition. A positive feature of incomplete demagnetization may be only reduced losses of remagnetization and, therefore, faster response, especially at the beginning of the process.

The residual flux intensity, when the current is reduced to zero, is assessed with the involvement of the notion of the partial loops of the static hysteresis. The residual flux intensity is determined with the accuracy sufficient for practical assessment using the ratio resulting from geometrical similarity of the fractional curves:

$$B_r^{real} = B_r \cdot B_{max}^{real} / B_{max}^{real}, \quad (11)$$

Fig. 10 compares the FRSA behavior depending on a varied organization of the process completion: with complete demagnetization and without it.

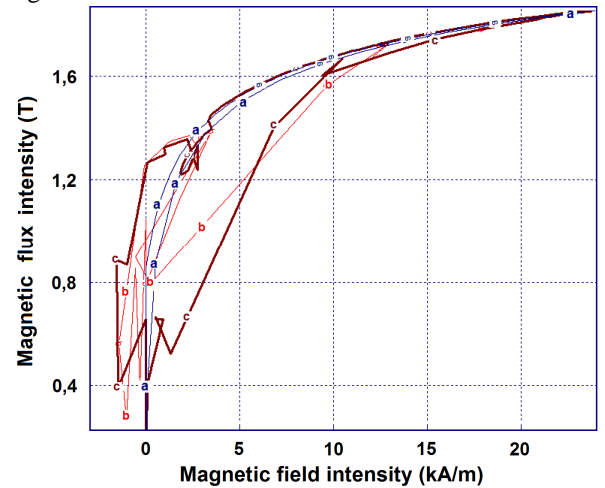


Fig. 10. Boundaries of static (a) and dynamic hysteresis with organization of the process without complete demagnetization (b) and with demagnetization (c)

In both cases, the current was completely hidden. The case of movement of the anchor with intensive motion damping from the side of the fuel spreading in the transverse direction along the clearance 0.05...0.12 mm is considered. Even with limitation of the magnetization parameter changing rates, the hysteresis loop area considering the effective magnetic field intensity is higher than in computation of the static hysteresis. It limits fast response of the valve and injector.

With higher rates of parameter changes – both electrical and hydromechanical, the dynamic hysteresis loop areas increase (Fig. 11). At the same time, when the FRSA is in operation, the value and sign of the  $dB/dt$  derivative are repeatedly changed, creating a wide range of possible values.

Organization of the process with or without demagnetization as well as computational analysis of the process within the static and dynamic hysteresis affects the final result – the dependences of the motion of the injector control valve. Thus, no demagnetization within the quasi-stationary analysis results in slowing down of the valve opening, i.e. return of the valve in the initial position (comparison of the a and g curves in Fig. 12). An attempt to compensate the valve closing period by means of tightening the return spring results in slower opening of the valve. Faster FRSA response with no demagnetization within the quasi-stationary analysis is not observed. Therefore, the conclusion is made that for faster response, complete demagnetization should be ensured.

Within consideration of the dynamic hysteresis, the role of demagnetization availability or nonavailability (h and i curves) is perceived as the same. In fact, magnetization does not improve the FRSA fast response when the valve is opening but worsens it when the valve is closing. Therefore, the conclusion that demagnetization is important holds true.

The unconditional regularity illustrated by Fig. 12 is as follows: consideration of the dynamic hysteresis has a strong impact on the final results related to the dynamics of the control valve movements. Namely, its response period increases both when opening and closing (a – h curves). Therefore, for more accurate prediction of the valve dynamics, it is necessary to take the dynamic hysteresis into consideration.

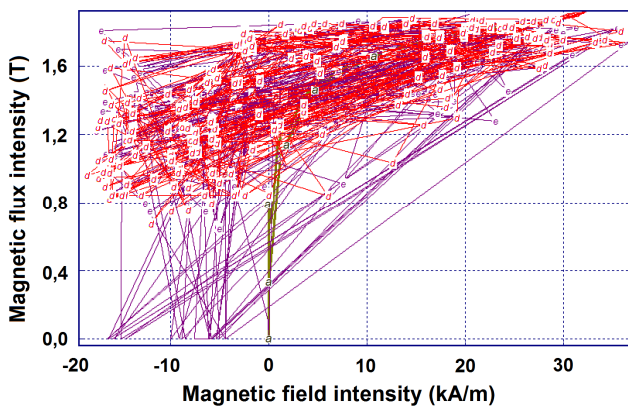


Fig. 11. Instantaneous flux intensity in magnetic core depending on effective magnetic field intensity: a – quasi-stationary (static) field intensity; d – effective (dynamic) field intensity without complete demagnetization; e – effective field intensity with demagnetization

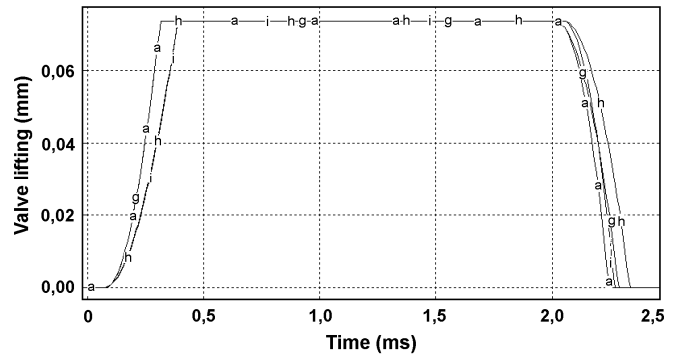


Fig. 12. Control valve lifting with the FRSA anchor in time function in different conditions of computation and process organization (computation in INJECT, current as per Fig. 3): a – static hysteresis, complete demagnetization; g – static hysteresis, no demagnetization; i – dynamic hysteresis, complete demagnetization; h – dynamic hysteresis, no demagnetization.

It is especially important to consider the FRSA response delay when calculating a short process, namely, small cycle injections. The situation is characterized with short periods of time when the valve is stopped (in the maximum stroke position). In such event, the main process time is spent on valve lifting and lowering (Fig. 13) and their motion computation error changes the process phase and fuel injection characteristics.

Special importance of the accurate computation of small injections is determined by several factors:

- well-known problems of small injection unevenness by the engine cylinders, engine vibrations, increased harmful emissions, and complete cylinder cutouts;
- extended use of multiple injections (Fig. 4) with several small injections.

Thus, in respect to the diesel engine of the motor truck with the nominal cycle injection of 165 mg, the pilot fuel batch with the accumulator pressure of 100 MPa has to be 8 mg. In such event, the injector needle does not reach its stop position and the valve may reach or may not reach the stop position.

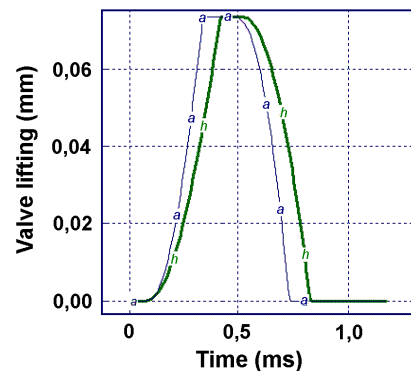


Fig. 13. Control valve lifting with the FRSA anchor in time function when computing with consideration of static (a) hysteresis and dynamic (h) hysteresis (computation in INJECT, no demagnetization)

Differences in the computations of the control valve motions with FRSA and fuel injection pressures within different methods of the computational organization in the INJECT software are demonstrated in Fig. 14. It should be noted that the cycle injection dispersion in this instance was 168%: from 4.96 mg to 13.3 mg.

Therefore, to make the injector response quicker, it is preferable to organize complete demagnetization of the magnetic core, not being limited only to reducing the current to zero. However, this recommendation is not mandatory: the injector may be operable without it as well, but with a somewhat slower response. At the same time, when calculating the FRSA performance, it is strongly recommended to consider the dynamic hysteresis.

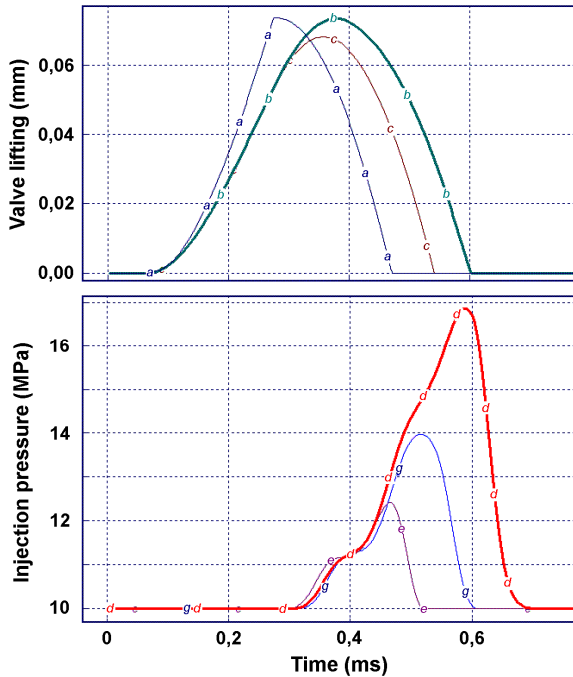


Fig. 14. Valve lifting and injection pressure when pilot batch is injected in time function: a, e – static hysteresis, magnetic core is demagnetized; c, g – dynamic hysteresis, magnetic core is demagnetized; b, d – dynamic hysteresis, no demagnetization.

### V. CONCLUSIONS

- The proposed approximation methods for the static hysteresis curves ensure agreement with the experimentally obtained curves for the steels used in the FRSA magnetic cores

of the engine fuel equipment. At the same time, they are simple for the computations and based on the parameters available in the reference books for the magnetic materials.

- The proposed integral method for computation of the processes in the FRSA is much simpler than the calculations involving 3D-simulation but delivers a sufficient level of the end result accuracy. It is built in the INJECT software for computation of the fuel injection equipment and used for the computational analysis and optimization of the system as a whole.

- The dynamic hysteresis in the fast process of remagnetization in the FRSA is much wider than the quasi-static one. It slows down the process and impedes the actuator fast response. For these reasons, it is mandatory to consider the effects of eddy currents and magnetic viscosity when calculating and designing the FRSA of the engine fuel systems.

- It is especially important to consider the FRSA response delay when calculating a short process, namely, small cycle injections and multiple fuel injections.

- To make the FRSA response faster, it is desirable to provide complete demagnetization of the magnetic core, not being limited only to reducing the current to zero.

### REFERENCES

- [1] P. Liu, L. Fan, D. Xu, X. Ma et al, "Multi-Objective Optimization of High-Speed Solenoid Valve Based on Response Surface and Genetic Algorithm," Presented at SAE Technical Paper 2015-01-1350, 2015, doi: 10.4271/2015-01-1350. [Online]. Available: <http://papers.sae.org/2015-01-1350/>
- [2] A.I. Kadochnikov "Dynamic reversal of magnetic electrical steel under the influence of stress of various shapes," Electricity, no. 9, pp. 62-66, September 2003.
- [3] J. Zhao, "Creating a fuel system equipment with control solenoid valve for future transport diesel engines", Ph.D. dissertation. Bauman Moscow State Techn. Univ, Moscow, RU, 2013.
- [4] L. Grekhov, K. Mahkamov, A. Kuleshov "Optimization of Mixture Formation and Combustion in Two-stroke OP Engine Using Innovated Diesel Spray Combustion Model and Fuel System Simulation Software," Presented at SAE Technical Paper 2015-01-1859, 2015, doi: 10.4271/2015-01-1859. [Online]. Available: <http://papers.sae.org/2015-01-1859/>
- [5] L.V. Grekhov, I.I. Gabitov, A.V. Negovora "Design, Computation and Technical Service of Fuel Equipment of Modern Diesel Engines: Textbook". – Moscow, RU, 2013, : Publishing House of the Legion Autodata, 2013, ch. 4, pp. 139-187.